Journal of Thermal Analysis and Calorimetry, Vol. 86 (2006) 3, 733–738

PLASMA SYNTHESIZED NANO-ALUMINUM POWDERS
Structure, thermal properties and combustion behavior

Alla Pivkina[1*], *D. Ivanov*[1], *Yu. Frolov*[1], *Svetlana Mudretsova*[2], *Anna Nickolskaya*[2] *and J. Schoonman*[3]

[1]Semenov Institute of Chemical Physics, Russian Academy of Science, Moscow, Russia
[2]Moscow State University, Department of Chemistry, Moscow, Russia
[3]Delft Institute for Sustainable Energy, Delft University of Technology, Delft, The Netherlands

The plasma electro-condensation process was used to synthesize nano-sized aluminum powders. Adding different chemicals modified the physical and chemical properties of these powders. To characterize the nano-sized powders, X-ray diffraction, TEM, BET analyses, and simultaneous TG/DSC analyses were performed. TG/DSC analyses revealed a dramatic degradation of the aluminum oxide layer after storage of the aluminum powder in air for a period of several months. The burning rate of the model solid propellant with nano-sized aluminum was experimentally examined. The combustion behavior of nano-sized aluminum will be presented and will be compared with the combustion behavior of the micron-sized powders.

Keywords: *aluminum powder, combustion, DSC, nano-particles*

Introduction

In the past, the transition from the millimeter-scale of particles to the micrometer-scale was of interest, whereas nowadays the nano-sized components are of interest in order to achieve high performance in rocket propellants and pyrotechnics. Nano-aluminum represents an example of such a material. It is expected that in comparison with the micron-sized particles, nano-sized aluminum powder will increase the burning rate, and will considerably decrease the agglomeration enhancing the specific impulse of solid rocket propellants. Metal particle agglomeration at the combustion surface is considered to be a reason for the metal particle ignition delay, chemical incompleteness of combustion, and the total efficiency losses. Experimental data show that the burning rate is strongly dependent on the component's sizes, and could be increased considerably by going down in size to the nano-scale [1–6].

Aluminum nano-particles can be prepared using a variety of techniques, including dynamic gas condensation [7], the cryomelting process [8], and by the plasma explosion process [9]. A thin native aluminum oxide layer on the nanoparticles occurs in air. This passivating oxide layer prevents fast aluminum oxidation during combustion, as well as agglomeration problems. To increase the reactivity of the oxide layer, different types of doping materials were used (Zn, Cu, Ni, Cr, Zr, alkali-earth metals, etc.). Characterization of the particle diameters, size distributions, oxide layer thicknesses, morphology of the particles, thermal behavior, and combustion parameters is important in predicting performance for specific applications. This paper reports on the experiments and the evaluation of the oxidation of nano-aluminum synthesized by the plasma electro-condensation technique. Different types of nano-aluminum powders are investigated, i.e., barium-doped nano-powder, benzine and silicon rubber stabilized powders. Barium-doped nano-aluminum is studied as received and aged during several months. Comparison of thermal and combustion behavior is made to the conventional Al micron-sized powder.

Experimental

Materials

Micron-sized aluminum powder with a spherical particle of average diameter of 10 μm was used as a reference powder and as a precursor for the plasma-synthesis process, which results in nano-sized Al powder. During the plasma-synthesis process, the argon gas flow delivers the precursor powder with additives to an argon-filled reactor, where aluminum powder evaporates in a high-temperature plasma zone. Details of the plasma-synthesis process have been reported elsewhere [1]. To increase the aluminum chemical reactivity, 1.5 at% of barium, which is equivalent to 7.5 mass% Ba, was added to the green

* Author for correspondence: alla_pivkina@mail.ru

1388–6150/$20.00

Akadémiai Kiadó, Budapest, Hungary
Springer, Dordrecht, The Netherlands

Table 1 Composition, specific surface, and active aluminum content of the investigated as-received samples

Sample	Composition mass/%	Specific surface/m^2 g^{-1}	Active Al content/%
1	Al+7.5% Ba	22.7	70.0
2	Al+1.5% benzine	9.1	88.3
3	Al+1.5% silicone rubber	9.1	75.0

Table 2 Aging periods of the investigated nano-powders (sample 1)

Sample	Composition	Aging period/months
1	Al+7.5% Ba	As-received
1.1	Al+7.5% Ba	3
1.2	Al+7.5% Ba	4
1.3	Al+7.5% Ba	4
1.4	Al+7.5% Ba +Pt-foil	4

powder mixture. Subsequent condensation of metal vapor represents nano-sized aluminum powder fabrication. For the current research three types of nano-particles were produced and investigated (Table 1). Samples 2, 3 contain stabilizing compounds, which were added after condensation.

Additionally, nano-aluminum powder containing 7.5% Ba was aged at 69% relative humidity, as listed in Table 2. The thermal behavior of aged samples was monitored continuously throughout the period. Different heating rates were applied to study the thermal behavior of samples 1.2 and 1.3, i.e., 10 and 2°C min^{-1}, respectively. Special experiments were performed to study the process of the nano-aluminum oxidation in the presence of Pt-foil to study the oxidation catalysis in a nano-sized powder.

Methods

Wet chemical analysis was performed to find the amount of active aluminum. It is a selective reaction between aluminum and water in the presence of sodium hydroxide. From the volume of hydrogen measured by displacement of water in a burette, the amount of active metal is calculated.

The Brunauer–Emmett–Teller (BET) method was used to determine the specific surface area [10].

X-ray diffraction patterns were obtained at room temperature using a Rigaku 'Geigerflex' X-ray diffractometer, employing CuK_α radiation. Samples were finely ground; the diffraction angle of 2θ was scanned at a rate of 2° min^{-1}. The average particle size was calculated by using the Sherrer's equation.

Transmission electron microscopy (TEM) microanalysis (JEM-2000 EX-II) was used as an independent method for characterization of the chemical composition and particle morphology. Analyses were performed at acceleration voltage of 200 kV. Various electron microscopy methods – bright- and dark-field TEM and microdiffraction were applied.

TG/DSC experiments were carried out using a Netzsch Simultaneous Thermal Analyzer STA 409. Experiments were conducted in static air. Approximately 10–20 mg of sample and reference material (α-Al_2O_3) were placed in separate alundum crucibles. Heating rate studies were conducted; samples were heated from 20 to 1100°C at 2 or 10°C min^{-1}. Calibrations of TG mass, DSC baseline, and temperature were conducted before the experiments.

The experimental investigations of burning rate and combustion of stoichiometric compositions of aluminum with ammonium perchlorate (AP) were conducted using a constant volume bomb pressurized with nitrogen. Samples were pressed tablets made of micron-sized ammonium perchlorate mixed with (*i*) micron-sized aluminum (sample 4), (*ii*) aged Ba-doped nano-aluminum, and (*iii*) benzine or silicon rubber stabilized nano-aluminum. The relative density of pellets was 90–98% of theoretical maximum density. The size of the pellets was 8 mm in diameter and 10–15 mm in length. Three cylindrical tablets were glued together to form one sample to increase the measurement accuracy. Data from three different experiments were averaged. In order to produce linearly burning tablets, the sides of each sample were inhibited with two-part epoxy. An electric match was taped on the top of the ignition mixture, which was painted onto the top of the sample. The calculated average accuracy of the burning rate measurements is ±5%.

The ignition was conducted using an electrically heated Ni–Cr wire set on top of the pellet. The combustion wave propagation was recorded with a video camera through a transparent quartz window. A data acquisition board L-154 was used to collect the measuring data to PC.

Results and discussion

Chemical purity, particle size and morphology

Table 1 presents the BET specific surfaces and the active aluminum contents of the investigated powders. As revealed by X-ray analysis, sample 1 contains the only one crystalline phase – aluminum metal. Considering the immediate reaction of barium to form an oxide layer BaO in air, barium oxide and barium were

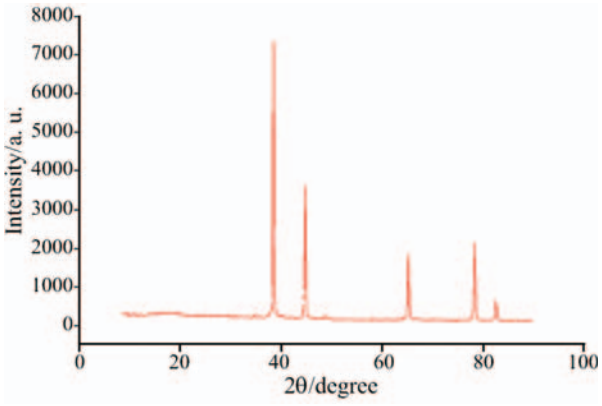

Fig. 1 X-ray diffraction pattern of sample 1 (nano-aluminum powder doped with 7.5 mass% Ba, as received)

expected to be present in the sample. Nevertheless, no indications of any crystalline Ba compounds were found, which is shown in Fig. 1. The active Al content is 70% (Table 1), therefore, 30% of as-received powder is supposed to be amorphous material comprising alumina and barium oxide. The average sizes of Al nanoparticles, determined from XRD line broadening, were 45 (111), and 41 nm (200).

The nano-sized Al particles were visualized by TEM. A picture from sample 1 is shown in Fig. 2a, and the particle size distribution calculated from twelve TEM images is plotted in Fig. 2b. The particles are ideally spherical with a Gauss particle-size distribution revealing an average particle diameter of 43 nm. Assuming that particles within a particular size fraction are coated by a passivating oxide layer of the equivalent thickness (ΔR_0), the ΔR_0 value was found to be 3.3 nm, which is close to the literature value of 2 to 4 nm [11–13]. Note that according to Auger spectroscopy, the real structure of the passivating oxide layer on the surface of an Al particle at room temperature is more intriguing. Under the aluminum oxide layer of about 3 nm thickness, a transition layer of about 10 nm thickness was detected, where the aluminum oxide molecules were found along with the Al metal atoms.

TG-DSC results

As-received powders

TG scans of as-received aluminum nano-powders in static air are shown in Fig. 3a. Initial mass loss due to adsorbed moisture of a few percent is seen below 300–400°C. Smaller particles of doped nano-aluminum would be expected to react at temperatures of 450°C, where the slow mass gain starts. The mass gain for sample 1 increases dramatically around 510°C: nano-particles oxidize very fast, in a regime similar to a thermal explosion. Indeed, the oxidation rate (DTG) for sample 1 is quite high, whereas for the

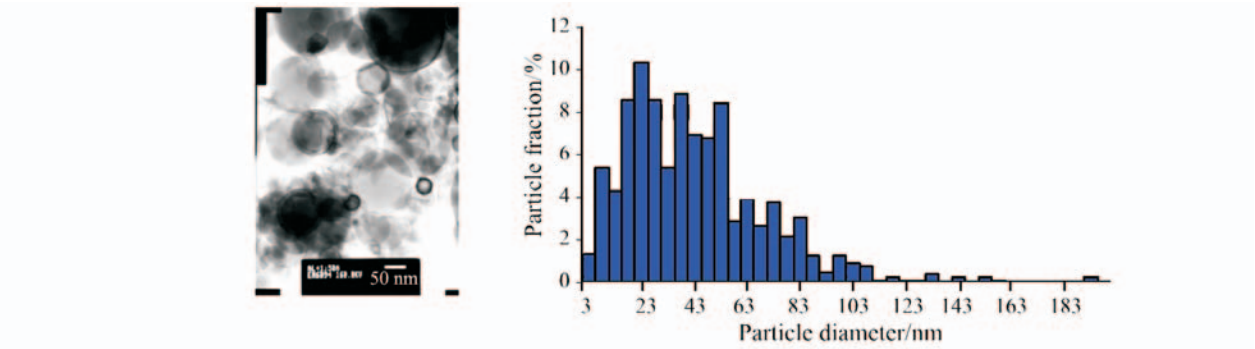

Fig. 2 TEM images of sample 1 (nano-aluminum powder doped with 7.5 mass% Ba, as received) with the particle size distribution obtained by TEM. Bar at the TEM image corresponds to 50 nm

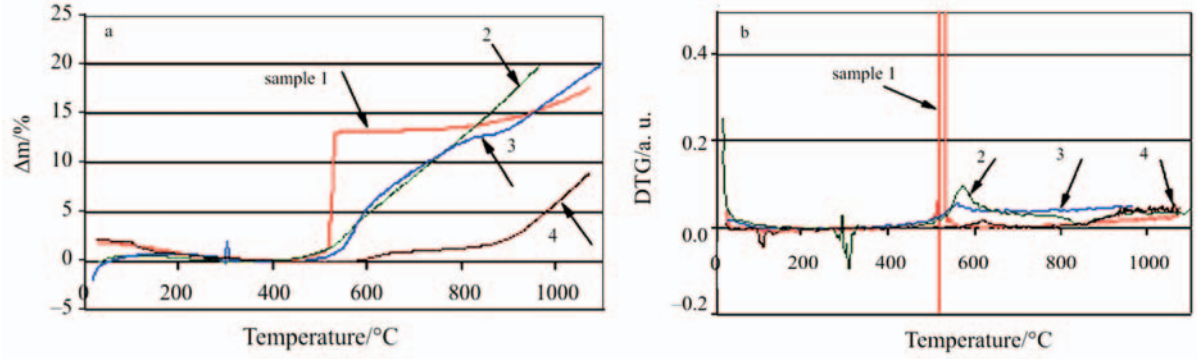

Fig. 3 a – TG and b – DTG traces of as-received aluminum powders showing rapid mass gain above 500°C for doped powder: sample 1 – Al+7.5% Ba, 2 – Al+1.5% benzine, 3 – Al+1.5% silicon rubber and 4 – micron-sized Al

Table 3 TG results of aluminum nano-powder oxidation

Sample	Heating rate/°C min^{-1}	T_1/°C	T_{max}/°C	m_1/%	$m_{1\,Al}$/%	T_2 /°C	m*/%	m^*_{Al}/%
1	10	516	527	12.97	20.89	820	17.6	28.35
1.1	10	512	567	14.47	23.31	640	45.25	72.89
1.2	10	530	580	27.79	44.76	666	51.43	82.85
1.3	2	490	540	30.81	49.63	636	52.78	85.02
1.4*	10	495	540	41.13	60.00	–	–	–
2	10	530	566	6.65	8.49	650	24.51	31.28
3	10	560	580	8.12	12.21	831	19.15	28.78
4	10	571	610	1.09	1.65	825	7.09	11.88

*sample was fast cooled at 630°C

samples 2, 3, 4 this value is much lower, as illustrated Fig. 3b. Noticeable oxidation of micron-sized aluminum (sample 4) starts above 800°C.

Table 3 summarizes TG results, i.e., the first oxidation onset temperature (T_1), the maximum oxidation rate temperature (T_{max}), the mass gain at the first peak (m_1), the amount of active metal reacting at the first oxidation step (m_{1Al}), the onset temperature for the second oxidation step (T_2), the total mass increase (m*), and the amount of active metal reacting at temperatures below 1100°C (m^*_{Al}). The total amount of oxidized aluminum m^*_{Al} of as-received nano-aluminum samples is found to be equivalent for as-received nanopowders (about 30%), but the thermal behavior of these powders is completely different. Indeed, sample 1 shows the very fast one-step oxidation at 510°C, followed by a TG-plateau until 950°C, whereas samples 2, 3, continuously react slowly with oxygen upon increasing temperature.

The fast oxidation of nano-aluminum doped with Ba at 510°C could be attributed to rapid diffusion of oxygen through the oxide layer after barium oxide's fast exothermical oxidation to form barium peroxide [14]. Arising considerable structural changes along with the additional heat release, may cause the oxide layer to crack at this temperature, thus causing a rapid increase in oxidation.

Assuming that after the first oxidation step (below the melting point 660°C) a 'new' passivating oxide layer on the particles of sample 1 has an equivalent thickness (ΔR_1) for the particles within a particular size fraction, the ΔR_1 value was calculated to be of 2.0 nm. Thus the total oxide layer thickness is 5.3 nm.

Aged nano-aluminum doped with Ba

Nano-aluminum powders doped with barium were aged at room temperature and 69% relative humidity in air using a closed can. The aging process of four months was followed using a TG/DSC thermal analysis. Results are compared in Fig. 4, where TG and DTG curves are presented. After 3 months of aging,

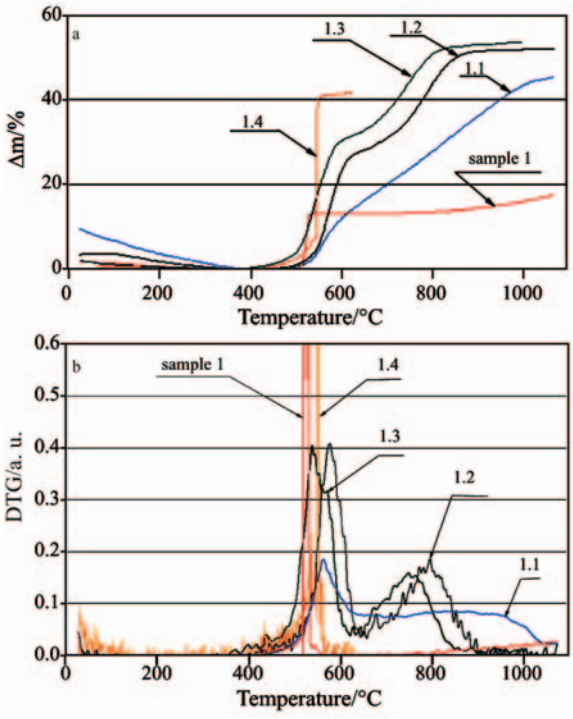

Fig. 4 a – TG and b – DTG traces of Ba-doped nano-aluminum showing the differences in the oxidation rate of Al+7.5 mass% Ba: sample 1 – as-received, 1.1 – aged for 3 months, 1.2 – aged for 4 months, 1.3 – aged for 4 months, heating rate is 2°C min^{-1}, 1.4 – aged for 4 months with Pt-foil doped powder: sample 1 – Al+7.5% Ba, 2 – Al+1.5% benzine, 3 – Al+1.5% silicon rubber and 4 – micron-sized Al

the doped nano-aluminum (sample 1.1) oxidizes continuously and the total amount of reacted metal (72.89%) is much higher than that of as-received sample 1. This indicates that an aluminum oxide layer degradates during storage dramatically, which could be caused by active interaction between barium oxide and humid air components.

Further storage of doped nano-aluminum (sample 1.2) leads to increasing of the oxidation rate, and obvious appearance of the second oxidation step at temperature around 800°C, which is shown in Fig. 4b. To

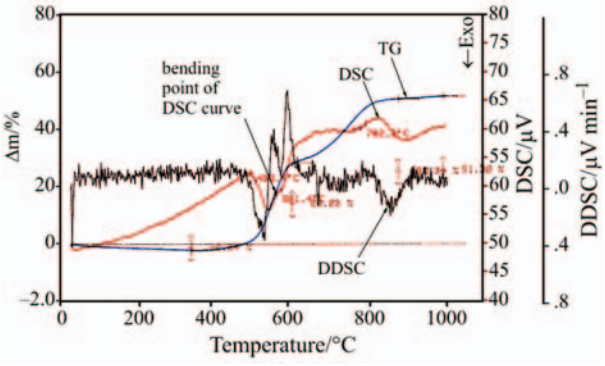

Fig. 5 TG-DSC-DDSC traces of Ba-doped nano-aluminum aged for 4 months (sample 1.3). Heating rate is 2°C min^{-1}

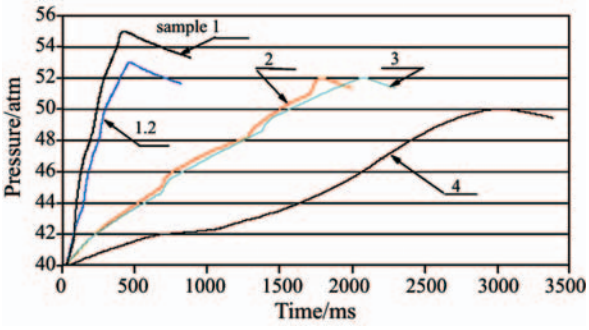

Fig. 6 Pressure history for the investigated compositions AP/Al with the different Al powders: sample 1.1 – Al+7.5% Ba, aged for 3 months; 1.2 – Al+7.5% Ba, aged for 4 months; 2 – Al+1.5% benzine; 3 – Al+1.5% silicon rubber; 4 – micron-sized Al. The initial pressure of nitrogen is 4 MPa

study the first oxidations step in more detail the TG/DSC experiment was repeated with a lower heating rate of 2°C min^{-1}. Figure 5 shows that the exothermal peak of the first oxidation step is formed by overlapping of several peaks; the temperature of 561°C corresponds to the bending point, as was found by DDSC analysis. In this sample particles that are larger or have thicker oxide layers oxidize later than smaller ones.

To study the chemical composition of the first oxidation step products, sample 1.2 was heated up to 630°C and than cooled very fast. Using a computer code 'Phan%', the crystal phase of the reaction product was found to comprise 59.7% of metal Al, and 40.3% of γ-Al_2O_3. The amounts present were quantified by thermogravimetric and X-ray diffraction methods and are presented in Table 4.

It seems, therefore, that the aging of Ba-doped nano-aluminum powder in humid atmosphere increases its oxidation rate at temperature around 500°C. This fact reflects the degradation process of the passivating oxide layer covering the nanoparticles.

Pt-catalyzed oxidation

As an oxidation catalyst, a platinum foil was used being crushed to form pieces and mixed with the powder to be investigated. Figure 4a shows TG results of the catalyzed nano-aluminum oxidation (sample 1.4). At temperature of 540°C a very fast 'thermal explosion' reaction is observed; the mass increase being found to be 41.13%, which corresponds to the oxidation of 60% of the active metal. The heat release at this particular temperature is extremely high –11.4 kJ g^{-1}. To study the melting of nanoparticles below 660°C, the heating process was interrupted at 630°C, and the sample was fast cooled down to room temperature. No changes in the platinum foil were detected, indicating the catalytic character of the activated oxidation, and the absence of liquid aluminum on the surface of nano-particles at temperatures below the bulk melting temperature.

Obviously, the catalyzed oxidation regime needs to be further investigated in detail, because of the great interest for the solid propellants combustion, where the condensed phase temperature is close to 400–500°C.

Combustion behavior

The burning rate at initial pressure of 4 MPa was measured in a nitrogen atmosphere by two independent techniques, i.e., analyses of the pressure history, and digitized video-images.

Pressure histories are presented in Fig. 6. They show that the internal pressure for samples with Ba-doped nano-aluminum is built up four times faster than for samples with nano-aluminum, stabilized with benzine and silicon rubber; and about ten times faster than that of the samples with conventional micron-sized aluminum powder. Figure 7 shows the averaged U values for investigated samples. The use of Ba-doped nano-aluminum (samples 1.1 and 1.2) instead of micron-sized metal (sample 4) results in a burning rate increasing from 3.7 to 42.0 mm s^{-1}. The use of the benzine (sample 2) and silicon rubber (sample 3) stabilized nanopowders leads to a burning rate increase of about two times, as shown in Fig. 7.

Table 4 X-ray analysis and TG results of aged aluminum nano-powder oxidation (sample 1.2)

Temperature/°C	Active Al content/%	Amorphous phase content/%	γ-Al_2O_3/%	α-Al_2O_3/%
20 (XRD)	70	30	–	–
630 (XRD)	41.8	30	28.2	–
630 (TG)	38.7	in total 61.3 (crystallinity could not be defined)		

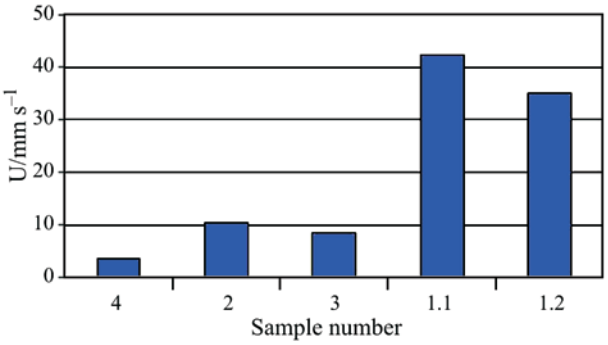

Fig. 7 Burning rate of stoichiometric compositions of 76% ammonium perchlorate and 24% aluminum with the different Al powders: sample 1.1 – Al+7.5% Ba, aged for 3 months; 1.2 - Al+7.5% Ba, aged for 4 months; 2 – Al+1.5% benzine; 3 – Al+1.5% silicon rubber; 4 – micron-sized Al. The initial pressure of nitrogen is 4 MPa

Conclusions

The present experiments provide the first comparison between the thermal behavior and combustion of different types of plasma-synthesized nano-aluminum and conventional micron-sized aluminum particles. Ba-doped nano-aluminum was found to have an average particle size of 43 nm, and an ideally spherical particle shape. Experiments show that the thermal behavior and combustion parameters of nano-aluminum are strongly dependent on the compounds being used during the particle fabrication process. Additionally, the considerable changes in the chemical activity of Ba-doped nano-aluminum were found during the powder storage, resulting in the oxide layer degradation.

Out of the studied series, the most suitable selected aluminum is Ba-doped powder, which is aged for 4 months, because of its high oxidation rate in air under heating, its high conversion degree in the temperature range 20–1100°C, and its considerable burning rate enhancement for the samples with ammonium perchlorate. Moreover, the process of Ba-doped nano-aluminum could be catalyzed by platinum metal: at temperature of 540°C a dramatic one-step oxidation of 60% of the active metal was found.

Acknowledgements

We wish to express our sincere appreciation to Prof. G. Pavlovetz (Petrovsky Scientific Center, Russian Academy of Rocket and Artillery Science) and Dr. A. Streletskii (Semenov Institute of Chemical Physics) for the experimental support. Financial support of the Russian Foundation of Basic Research (RFFI grant #04-03-32273a) is gratefully acknowledged.

References

1 G. Pavlovetz, Scientific and Technological Basics of Production and Use of Ultra-Sized Metal Powders for the High-Energetic Compositions, Section of Application Problems, Prezidium of Russian Academy of Science, Moscow 1999, p. 80.
2 A. Pivkina, Yu. Frolov, S. Zavyalov, D. Ivanov, J. Schoonman, A. Streletskii and P. Butyagin, Proceedings of Thirty-First International Pyrotechnics Seminar, Fort Collins, Colorado July 11–16, (2004) 285.
3 M. M. Mench, K. K. Kuo, C. L. Yeh and Y. C. Lu, Combust. Sci. Technol., 135 (1998) 269.
4 C. E. Aumann, G. L. Skofronick and J. A. Martin, J. Vac. Sci. Technol., B 13 (1995) 1178.
5 Y. Champion and J. Bigot, Nanostructured Materials, 10 (1998) 1097.
6 A. Pivkina, P. Ulyanova, Yu. Frolov, S. Zavyalov and J. Schoonman, Propellants, Explosives, Pyrotechnics, 29 (2004) 39.
7 H. C. Burger and P. H. Cittert, Z. Phys., 66 (1930) 210.
8 A. G. Goursat, G. Vernet, J. F. Rimpert, J. Foulard, T. Darle and J. Bigot, Metal powder manufacture starting with a molten material, Air Liquide SA pour l'Etude et l'Exploitation des Procèdes Georges Claude, France 1984, p. 9.
9 G. V. Ivanov, M. I. Lerner and F. Tepper, Adv. Powder Metall. Pat. Meter., 4 (1996) 15.
10 ASTM C1274-00, Standard Test Method for Advanced Ceramic Specific Surface Area by Physical Adsorption, 01/01/2000, American Society for Testing Materials, Conshohocken, PA, USA.
11 Mary Sandstrom, Betty Jorgensen, Bettina Smith, Joseph Mang and Steven F. Son, Proceedings of Thirty-First International Pyrotechnics Seminar, Fort Collins, Colorado July 11–16, (2004) 241.
12 R. Franchy, Surf. Sci. Reports, 38 (2000) 195.
13 X. Phung, J. Groza, E. A. Stach, L. N. Williams and S. B. Ritchey, Mater. Sci. Eng., A 359 (2003) 261.
14 I. Vol'nov, Peroxide Compounds of Alkali-Earth Metals (in Russian), Moscow, Nauka 1983, p. 136.

Received: August 24, 2005
Accepted: November 11, 2005
OnlineFirst: June 27, 2006

DOI: 10.1007/s10973-005-7300-9